1694
doi:10.1017/S1431927610060800
Microsc. Microanal. 16 (Suppl 2), 2010

A New Approach for the Quantitative Analysis of Degree of Dispersion of Clay Particles in the Polymer Matrix by Electron Microscopy Combined with Small-angle X-ray Scattering

Jayita Bandyopadhyay and Suprakas Sinha Ray

DST/CSIR Nanotechnology Innovation Centre, National Centre for Nano-Structured Materials, Council for Scientific and Industrial Research, Pretoria 0001, Republic of South Africa.

The main objective of this work is to propose a new approach for the quantitative analysis of the degree of dispersion of clay particles in the polymer matrix by small-angle X-ray scattering (SAXS) combined with electron microscopy. The dispersed structure of the clay particles in the poly[(butylene succinate)-co-adipate] (PBSA) matrix was studied by SAXS. The morphology of the nanocomposites was extensively studied by scanning transmission electron microscopy (STEM). In the case of all nanocomposites, SAXS results were in good agreement with STEM observations.

PBSA nanocomposites (PBSANC) with four different weight percentages of C30B loading were prepared via melt-mixing in a Polylab Thermohaake-batch mixer at 125°C with a rotor speed of 60 rpm. The PBSA nanocomposites (PBSANCs) with four different C30B loadings of 3, 4, 5, and 6 wt% were abbreviated as PBSANC3, PBSANC4, PBSANC5, and PBSANC6, respectively.

Fig. 1 shows the most representative bright-field STEM images of various PBSANCs in which black entities represent the dispersed silicate layers. The STEM image of PBSANC3 (Fig. 1(a)) shows that as a whole the clay particles are dispersed nicely in the PBSA matrix and the inter-particle distance is much higher than in the other model nanocomposites. Still there is some overlapping of neighboring particles, which increases the stacking of the clay layers. In the case of PBSANC4 (Fig. 1(b)), the dispersion characteristics are almost the same as PBSANC3; however, only the probability of finding neighbors increases.

To have deeper understanding of the degree of dispersion of silicate layers in PBSA matrix, Image J software was used to analyze STEM images. In Fig. 1(e), the number of stacked silicate layers (in %) for the different nanocomposites is plotted against the thickness of the stacked silicate layers (in nm) determined on the basis of the STEM images. It is clear from the figure that for all nanocomposites the minimum thickness of the dispersed silicate layers can be 1.5 nm. This result is relevant with the SAXS analysis. Furthermore, in the case of PBSANC3, the maximum number of the stacked silicate layers possess the thickness in a range of 4.5 −7.5 nm. In PBSANC4, the percentage of the silicate layers stacking falling in the first two thickness range reduces and the number of stacked silicate layers with higher thickness increases. From the STEM analysis, it is also prominent that for these two nanocomposites (PBSANC3 and PBSANC4) there is a drastic change in intercalated silicate layers' population in neighbouring thickness zone. While, in the case of PBSANC5, the silicate layers population of different thickness range does not change drastically. For PBSANC6, initially the population of silicate layers reduces in the first two thickness zone, but it suddenly increases within 7.5−10.5 and 10.5−13.5 nm. After fitting cubic splines on the histogram it is clear that the nature of the fitting curve changes from Lorentzian to almost Gaussian with increase in C30B loading. The intensity of the peak reduces systematically as the C30B concentration increases up to 5 wt%. Further increase in C30B concentration results higher intense peak. Therefore, it can be concluded that PBSANC5 has splashed cards like flocculated structure. On the other hand, because of the Gaussian fitting of the histogram one can say PBSANC6 possesses nicely dispersed stacked-intercalated structure. Again, the peak positions of mainly Lorentzian distributions (i.e., for PBSANC3 to PBSANC5) falls within the thickness range of 4.5-7.5 nm, i.e., on average 6 nm (see Fig. 1(e)). According to SAXS results, the mean number of layers (n) varies between 5.6–5.8 with the variation of clay content in the nanocomposites.

From the SAXS results, in the case of PBSANC3, the clay platelets are nicely delaminated since the probability of finding a neighbour is much less [1]. However, the probability of finding neighbouring particles at almost the same distances increases in the case of PBSANC4 as compared to PBSANC3. In the case of PBSANC5, the probability of finding neighbors increases both in the short and long distances. A tangent on the initial linear decaying portion can give a rough estimation of the largest single particle size (i.e., the smallest thickness of the dispersed clay layers) in PBSANC5 and it is ~1.5 nm. For PBSANC6, it is also ~1.5 nm. Therefore, PBSANC5 attains the maximum limit of delamination of clay layers and already the neighbours are overlapping like the flocculated nanocomposites' structure [2]. After that, due to the geometric constraints, it is not possible to delaminate clay layers anymore and the clay stacking increases as in the case of PBSANC6. Therefore, the SAXS observations support the conclusions made on the basis of the STEM analysis.

In conclusion, the STEM observations and SAXS results show that the amount of clay loading plays a vital role in controlling the network structure of dispersed silicate layers of nanocomposites and, hence, melt-flow behaviours of nanocomposites.

References

[1] O. Glatter, O. Kratky, Small Angle X-ray Scattering, Academic Press, London.
[2] S. Sinha Ray, K. Okamoto, K. Okamoto, *Macromolecules* 36 (2003) 2355.

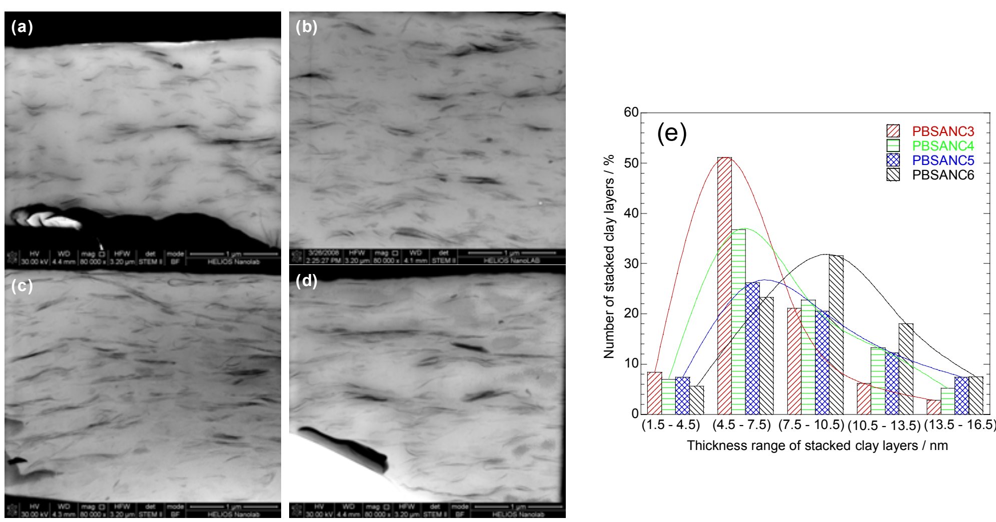

FIG.1. The bright-field scanning transmission electron microscopy (STEM) images of four different nanocomposite systems, in which black entities represent the dispersed silicate layers: (a) PBSANC3, (b) PBSANC4, (c) PBSANC5, (d) PBSANC6, and (e) the number of stacked silicate layers (in %) for the different nanocomposites is plotted against the thickness of the stacked silicate layers (in nm) determined on the basis of the STEM images.

https://doi.org/10.1017/S1431927610060800 Published online by Cambridge University Press